Population genomics reveals an ancient origin of heartworms in canids

Rosemonde I. Power[1], Swaid Abdullah[2], Heather S. Walden[3], Guilherme G. Verocai[4], Tiana L. Sanders[4], Joe L. Luksovsky[4], Andrew R. Moorhead[5], Michael T. Dzimianski[6], Jeremy M. Foster[7], Michelle L. Michalski[8], Alicia Rojas[9,10], Samuel C. Chacón[11], Georgiana Deak[12], Andrei D. Mihalca[12], Patrizia Danesi[13], Elias Papadopoulos[14], Piyanan Taweethavonsawat[15,16], Dung Thi Bui[17,18], Anh Do Ngoc[19], Reuben S.K. Sharma[20], Simon Y.W. Ho[21], Stephen R. Doyle[22,*+] and Jan Šlapeta[1,23,*+]

1. Sydney School of Veterinary Science, Faculty of Science, The University of Sydney, New South Wales, Australia
2. University of Queensland, School of Veterinary Science, Gatton, Queensland, Australia
3. Department of Comparative, Diagnostic, and Population Medicine, College of Veterinary Medicine, University of Florida, Florida, USA
4. Department of Veterinary Pathobiology, College of Veterinary Medicine & Biomedical Sciences, Texas A&M University, Texas, USA
5. Department of Clinical Sciences, College of Veterinary Medicine, North Carolina State University, Raleigh, North Carolina
6. Department of Infectious Diseases, College of Veterinary Medicine, University of Georgia, Athens, Georgia, USA
7. New England Biolabs Inc., Ipswich, Massachusetts, USA
8. University of Wisconsin Oshkosh, Oshkosh, Wisconsin, USA
9. Laboratory of Helminthology, Faculty of Microbiology, University of Costa Rica, San José, Costa Rica

10. Centro de Investigación en Enfermedades Tropicales, University of Costa Rica, San José, Costa Rica
11. Department of Veterinary Parasitology, Veterinary Sciences, Healthy Pet Veterinary Hospital SC, David, Chiriquí, Panamá
12. Department of Parasitology and Parasitic Diseases, University of Agricultural Sciences and Veterinary Medicine of Cluj-Napoca, Calea Mănăștur 3-5, Cluj-Napoca, Romania
13. SCS3 - Parasitology and Mycology Unit, Istituto Zooprofilattico Sperimentale delle Venezie, Viale dell'Università 10, Legnaro, Italy
14. Laboratory of Parasitology and Parasitic Diseases, Faculty of Veterinary Medicine, Aristotle University of Thessaloniki, Thessaloniki, Greece
15. Parasitology Unit, Department of Veterinary Pathology, Faculty of Veterinary Science, Chulalongkorn University, Bangkok, Thailand
16. Biomarkers in Animals Parasitology Research Unit, Chulalongkorn University, Bangkok, Thailand
17. Institute of Biology, Vietnam Academy of Science and Technology, Hanoi, Vietnam
18. Faculty of Ecology and Biological Resources, Graduate University of Science and Technology, Vietnam Academy of Science and Technology, Hanoi, Vietnam
19. Department of Medical Parasitology, Vietnam Military Medical University, Hanoi, Vietnam
20. Faculty of Veterinary Medicine, Universiti Putra Malaysia, Serdang, Selangor, Malaysia
21. School of Life and Environmental Sciences, Faculty of Science, The University of Sydney, New South Wales, Australia
22. Wellcome Sanger Institute, Hinxton, Cambridgeshire, UK
23. Sydney Infectious Diseases Institute, The University of Sydney, New South Wales, Australia

+ These authors jointly supervised this work.

* Corresponding authors.

E-mail address: jan.slapeta@sydney.edu.au (J. Šlapeta); stephen.doyle@sanger.ac.uk (S. Doyle)

Abstract

Heartworms (*Dirofilaria immitis*) are parasitic nematodes that cause significant cardiopulmonary-associated morbidity and mortality in canids worldwide. The global spread of heartworms is believed to have occurred alongside the dispersal of domesticated dogs. To test this theory, we analysed the genomes of 127 specimens collected from mammalian carnivore hosts across four continents. Here we show distinct genetic differences between heartworms from different continents, indicating a more ancient dispersal in canid hosts than previously recognised. Using admixture analyses, we find an Asian origin for Australian heartworms, consistent with the arrival of dingoes thousands of years ago. Finally, the genetic relatedness between European and Central American heartworms suggests that modern dispersal, likely associated with human colonisation of the Americas by Europeans, occurred with domesticated dogs. This work sheds light on the population dynamics and deep evolutionary history of a globally widespread parasite of veterinary significance.

Introduction

The canine heartworm, *Dirofilaria immitis*, is a parasitic nematode that infects a broad range of mammalian carnivores (order Carnivora) across tropical, subtropical, and temperate regions worldwide [1]. Mosquitoes transmit larval stages of heartworms, which develop after infection and reside in their host's heart and pulmonary arteries as adults [2]. These adult worms can cause lesions, vascular damage, pulmonary hypertension, and right-sided congestive heart failure, potentially leading to the death of their host [2]. This is of particular concern in domestic dogs, where the onset of disease can be prevented through the rigorous and lifelong application of parasiticides [3]. Such treatment regimes have led to the emergence of drug resistance [4,5] that, while currently only well described in the USA, threatens heartworm control globally if it were to spread. Heartworms are predicted to increase in prevalence and expand into new regions due to climate change, pet travel, and habitat alterations [6]. Therefore, defining the origins, distribution, and capacity for transmission will have important implications for implementing effective heartworm surveillance and control.

Current views on the evolutionary origins and subsequent radiation of heartworms worldwide are anthropocentric in nature. Heartworms are believed to have originated in Europe [7] or Asia [2] and spread globally over the past 200–400 years via human-mediated dog movements. Accordingly, heartworms are presumed to form a single homogeneous global population. While some studies have supported this hypothesis by demonstrating low diversity and limited population structure amongst heartworms [8–11], these studies had limited sampling, both in terms of numbers of sequences and geographic representation. The currently accepted view of a recent global dispersal also overlooks the deep co-

evolutionary history that many parasites have shared with their hosts and the environments in which they reside. The broad host range of heartworm potentially indicates a long co-evolutionary history with mammalian carnivores, especially canids [12,13], a group that dates back approximately 40 Mya [14], predating humans (~2.8 Mya) [15] and the domestication of modern dogs (14–40 kya) [16–18]. Given also that mosquito vectors, which are essential for heartworm transmission, have existed since the early Triassic (217 Mya) [19], it is possible that heartworms radiated long before human involvement. We propose that heartworms offer a compelling case for assessing the degree to which anthropogenic activities have influenced parasite distribution.

Analyses of genomic data have significant potential to identify the historical origins of heartworms and infer their global dispersal routes, as demonstrated for other helminths [20–22]. Sequencing adult heartworms is recommended for obtaining high-quality data [23]; however, obtaining adults from the heart requires invasive surgery or post-mortem, which are often not feasible. Such sampling is especially difficult in parts of Asia and Africa, where cultural perceptions of dogs as unclean or carriers of disease can restrict sampling opportunities. In light of these challenges, here we present the most extensive population genomics study of heartworms to date. Using whole genome sequencing of 127 adult worms obtained from nine countries on four continents, we analyse the diversity, genetic structure, and population demographics of modern heartworms to infer their historical origins and dispersal.

Our population genomic analyses of heartworm parasites reveal a global diversity that has been shaped by both ancient and recent biogeographic events. We observed strong continental population structure, likely influenced by the distribution of ancestral canid

111 hosts throughout time. We detected genetic admixture between Asian and Australian
112 heartworms, which coincided with the arrival of dingoes in Australia. We also provide
113 evidence of recent human-driven dispersal, potentially linked to the movement of
114 domesticated dogs from Europe to Central America during colonisation.

115

116 Results and Discussion

117 Genomic diversity of heartworms from multiple continents, countries, and hosts

118 We analysed whole-genome sequencing data from 127 adult heartworms (*Dirofilaria*
119 *immitis*) sampled from nine countries in five regions: Australia, North America (USA), Central
120 America (Costa Rica, Panama), Europe (Greece, Italy, Romania), and Asia (Malaysia,
121 Thailand) (Fig. 1a). Samples were primarily collected from domestic dogs (n = 115), but we
122 also sampled cats (n = 4), foxes (n = 4), a ferret (n = 1), a golden jackal (n = 1), a leopard (n =
123 1), and a wildcat (n = 1). Overall, we obtained an average coverage per sample of 75.47× for
124 the nuclear genome, 13,119.80× for the mitochondrial genome, and 1,047.09× for the
125 *Wolbachia* endosymbiont genome (Supplementary Data 1, Supplementary Fig. 1–4). Variant
126 calling, joint genotyping, and filtering of heartworm samples revealed 264,558 nuclear single
127 nucleotide polymorphisms (SNPs) (3.3 SNPs per kb), 32 mitochondrial SNPs (2.3 SNPs per
128 kb), and 280 *Wolbachia* SNPs (0.3 SNPs per kb). The SNP frequencies in the nuclear and
129 mitochondrial genomes are comparable, whereas the frequency in the *Wolbachia* genome is
130 considerably lower. These frequency data are comparable to those of other *Wolbachia*-
131 infected filarial worms, such as *Onchocerca volvulus* [24] and *Wuchereria bancrofti* [22].

132

133 **Nuclear variants reveal distinct continental partitioning of heartworms**

134 Analyses of the heartworm cohort's genetic diversity revealed distinct groups of samples
135 based on broad geographical regions. Principal component analysis (PCA) using 196,550
136 high-quality autosomal SNPs revealed four clusters of samples corresponding to the
137 continents from which the samples were collected (Fig. 1b and Supplementary Fig. 5; PC1
138 variance: 12.6%, PC2 variance: 10.69%). The third and fourth PCs showed a similar pattern
139 of geographical clustering (Supplementary Fig. 6a; PC3 variance: 5.76%, PC4 variance:
140 4.39%); however, although the signal was comparatively weaker, the European and Central
141 American samples formed separate clusters. Similar findings were observed in a previous
142 study of 31 heartworm samples from Australia, Italy, and the USA, where samples from each
143 country formed distinct clusters [25]. Independent PCAs of SNPs from each chromosome
144 found the same continental clustering pattern across all chromosomes, including the sex-
145 linked X chromosome (Supplementary Fig. 6b–f), suggesting that this is a genome-wide
146 rather than region-specific observation. The distinct geographical partitioning in our nuclear
147 data was not supported by the mitochondrial (Supplementary Fig. 7a) or *Wolbachia* data
148 (Supplementary Fig. 7b), likely due to the limited number of variant sites within each
149 dataset.

150 Analyses of genome-wide nucleotide diversity (Pi) further demonstrated differences
151 between heartworm populations across continents. Pi differed significantly between all
152 populations (Wilcoxon rank sum test, $P < 0.001$), with the exception of Europe and Central
153 America (Fig. 1c). The highest Pi was observed in the USA (Pi[mean] = 7.39×10^{-4}), while the
154 lowest was in Asia (Pi[mean] = 2.89×10^{-4}). The genetic diversity of our USA samples aligned
155 closely with that of a previous *D. immitis* study (Pi[mean] = 7.36×10^{-4}) [25]. However, our

156 Australian samples (Pi[mean] = 5.61×10^{-4}) exhibited higher genetic diversity than those
157 reported previously (Pi[mean] = 3.9×10^{-5}) [25], likely due to the larger and geographically
158 broader sampling here. Overall, the nucleotide diversity of our *D. immitis* samples is
159 comparable to that of the filarial worm *W. bancrofti* (Pi[mean] = 2.4×10^{-4}) [22] but lower than
160 that of *O. volvulus* (Pi[mean] = 4.0×10^{-3}) [24]. Each *D. immitis* population exhibited different
161 rates of linkage disequilibrium (LD) decay and baseline LD (Fig. 1d), with Asia and the USA
162 showing the highest and lowest LD, respectively. Estimates of admixture provided further
163 support for continental partitioning in heartworms. To infer the ancestry proportions of
164 samples, we used NGSadmix with a range of *K* clusters (*K* = 2–10; Supplementary Fig. 8). At *K*
165 = 6, Australian samples showed the most diverse admixture patterns with strong evidence
166 of shared ancestry with Asia, whereas USA, Europe, and Central America were largely
167 distinct with some evidence of shared ancestry in a minority of European and Central
168 American samples (Fig. 1e). The strong population structure in the nuclear genome of
169 heartworms suggests that spatial spread has been restricted during the species' history,
170 resulting in distinct genetic profiles on each continent.

171

172 **Inference of transmission between diverse heartworm hosts**

173 Heartworms are obligate, vector-borne parasites whose successful establishment in a new
174 environment depends on three key requirements. The first requirement is the presence of a
175 suitable definitive host in which heartworms can develop, establish in the pulmonary
176 arteries and the heart, and sexually reproduce to generate microfilariae, which circulate in
177 the host's bloodstream. The second requirement is a suitable mosquito vector that can
178 ingest the microfilariae and support their development until they reach their infective larval

179 stages. The final requirement relates to the conditions needed for larval development
180 within the mosquito, which is both temperature- and time-dependent. Assuming a 30-day
181 life expectancy and ingestion of heartworm microfilariae on Day 1, mosquitoes would
182 require a minimum mean daily temperature of 19.3°C throughout the entire month for the
183 larvae to develop into their infective stages and become transmissible to the next host [26].
184 Warmer climates would accelerate this developmental stage inside the mosquito vector.
185 This complex interplay between host, vector, and climate has enabled heartworms to infect
186 both domestic and wild animals on almost every continent of the world.

187 Although most heartworm samples in this study were obtained from dogs, the
188 analysis of heartworm genomes from foxes, cats, a golden jackal, a ferret, and a leopard
189 allowed us to evaluate genetic variation among different host species. We found that
190 geography rather than the host species explained variation in the global heartworm
191 population, evidenced by samples from cat and ferret nested within samples from dogs in
192 the USA, fox and dogs in both Australian and Italian groups, and dogs and jackal, wildcat and
193 leopard from Europe (Fig. 2a). Analyses of nucleotide diversity (Pi), absolute nucleotide
194 divergence (D_{XY}), and genetic differentiation (F_{ST}) provided additional insights on the
195 variation within and between different host species. The heartworm sampled from the
196 ferret had the highest diversity (Pi[mean] = 1.21×10^{-3}) (Fig. 2b) and the greatest divergence
197 from other hosts (Supplementary Fig. 9a). In contrast, the samples from the golden jackal,
198 leopard, and wildcat had the lowest diversity (Pi[mean] $1.10–1.89\times10^{-4}$) and were the least
199 divergent from each other compared with all other host pairs. However, only a single
200 heartworm was sampled from each of these hosts, and the variation observed in the jackal,
201 leopard, and wildcat samples may be confounded as they all originated from Romania. F_{ST}
202 values between host pairs were generally low, with foxes showing the highest genetic

203 differentiation from other hosts, except for the domestic dog (Supplementary Fig. 9b).
204 Collectively, these data suggest an absence of obvious host-specificity and that transmission
205 is likely between domestic animals and wildlife. However, further geographic sampling from
206 non-dog hosts is needed to exclude the possibility of host-specific adaptation.

207 We next questioned which host may have harboured and dispersed heartworms
208 before the emergence of modern dogs. We hypothesised that longer co-evolution between
209 parasites and hosts would result in the latter being able to carry higher parasite loads. Felids
210 (e.g. domestic cats, wild cats, snow leopards), procyonids (e.g. raccoon dogs), mustelids (e.g.
211 European badger, ferrets), pinnipeds (e.g. harbour seal, brown fur seal), and ursids (e.g.
212 brown bear, black bear) have been described as being infected with heartworms
213 (Supplementary Table 1); however, they typically carry fewer adult worms and fail to
214 support the parasite's entire life cycle, and so they are not considered primary reservoirs [27–
215 30] (Fig. 3b). In contrast, wild canids are commonly microfilaremic and have high worm
216 burdens. Wolves and coyotes have worm burdens similar to dogs, while jackals and foxes
217 have significantly lower burdens than dogs (Kruskal-Wallis test with Dunn's multiple
218 comparisons; Dog vs Jackal: $P \leq 0.05$, Dog vs Fox: $P \leq 0.001$) (Fig. 3b). These findings imply
219 that canids, particularly ancestral wolves or coyotes, were most likely the primary hosts for
220 heartworm during ancient times [31].

221

222 **Coevolution of canids and heartworms: distinguishing modern from ancient origins and**
223 **dispersal**

224 Previous work had proposed that canids originated in North America ~40 Mya when the
225 continent was completely isolated [14], whereas mosquitoes originated much earlier in the

226 Triassic (~217 Mya) [19]. Phylogenetic analyses of mitochondrial DNA suggest that heartworms
227 diverged from their closest relatives in the genus *Onchocerca* ~25 Mya during the Oligocene
228 [32], i.e., when canids and mosquito vectors were already well-established. Together, this
229 timeline supports a long co-evolutionary history between heartworms and ancient canids.

230 The formation of the Bering Land Bridge and the Isthmus of Panama during the
231 Miocene and Pliocene facilitated the first migrations of canids into Eurasia (~7 Mya) [14] and
232 South America (3.5–3.9 Mya) [33], respectively. Throughout history, fluctuations in sea level
233 have repeatedly exposed and submerged the Bering Land Bridge. Fossil records and
234 genomic data provide robust evidence that these periods of exposure allowed ancient
235 canids to form contiguous populations across the Northern Hemisphere. Examples include
236 Pleistocene wolves, which were highly connected across North America and Eurasia [16,34,35],
237 *Xenocyon lycaonoides,* a large canid distributed across North America and Eurasia in the mid
238 Pleistocene [36] and *Eucyon,* a jackal-sized canid distributed across North America, Eurasia,
239 and Africa in the late Miocene [37]. The existence of these interconnected ancient canid
240 populations suggests that heartworms may have formed a highly connected population with
241 their hosts at that time.

242 The current hypothesis for the distribution of heartworms around the world is that it
243 has been largely influenced by human movement in contemporary times. Alternative
244 hypotheses suggest that heartworms spread with humans during or shortly after dog
245 domestication (~14–40 kya), or that they spread with wild canids before domestication. To
246 further explore the demographic history of heartworms, we inferred their effective
247 population (Ne) size histories using SMC++ over the last 1 million years. Given the
248 domestication hypothesis, we broadly characterise the population demographics into three

249 periods: post-domestication (<14 kya), domestication (14-40 kya), and pre-domestication
250 (>40 kya). Contemporary estimates of Ne after domestication (Figure 3a) were consistent
251 with current levels of genetic diversity (Figure 1c) in each population, with USA and
252 Australian populations showing the highest Ne and Pi, and Asia the lowest. Differences
253 between populations in demographic analysis broadly support the D_{XY} and F_{ST} results
254 (Supplementary Fig. 10), which indicate the greatest differentiation and, therefore, infer
255 population splits from Asia, which diverged from the populations of Europe, the USA, and
256 Central America. Considering the variation in population demographic curves >40 kya
257 (Figure 3a), we propose that there were substantial differences in some populations that
258 were evolving independently before dog domestication [16–18]. Given that modern global
259 human movement would drive populations to be more similar, the exacerbation of
260 differences in Ne post-domestication would further suggest that these differences in
261 populations existed before domestication.

262 If heartworms were once one population, when did they diverge, and why? Our
263 estimates of Ne do not extend earlier than 1 million years ago. However, between 1 million
264 and ~50,000 years ago, significant climatic events correlate with changes in the heartworm
265 population demographics. For example, we observe a substantial increase in Ne of all
266 populations roughly aligning with the last interglacial period (Figure 3a), when Earth
267 experienced a climate as warm or even warmer than today (116–130 kya) [38]. Such an
268 environment could have been suitable for the development and transmission of
269 heartworms via mosquito vectors. Following the warm climates of the last interglacial
270 period, the Earth began to cool. By Marine Isotope Stage 4 (58–72 kya), large continental ice
271 sheets had formed across North America, Beringia, and northern Eurasia [39]. These ice sheets
272 separated ancient canid populations [34,40], potentially fragmenting the associated ancient

273 heartworm population. This time period was associated with a fall in Ne, particularly in the
274 USA samples, but for all populations, a considerable decrease was observed immediately
275 before or during dog domestication, which occurred shortly afterwards (Figure 3a). This
276 fragmentation would have reduced gene flow for extended periods, explaining the
277 continental grouping of samples in our study. Further insights might be obtained by
278 exploring the presence of heartworm DNA in the remains of ancient canids; if successfully
279 extracted, these ancient worm DNA sequences may fill in the temporal and geographic gaps
280 needed to understand heartworm divergence in more detail. Similarly, further sampling in
281 unstudied regions, including South America and Africa, and finer sampling within Asia,
282 would enhance our understanding of heartworms' evolutionary history.

283 Considering global warming and cooling cycles, the fragmentation of canid and
284 heartworm populations would have occurred multiple times. We found evidence of
285 secondary admixture between heartworms from Asia and the USA after the initial
286 population divergence, evident from both the admixture analyses and gene flow between
287 populations (Fig. 4a; delta m = 3.4; all tree migration edges are presented in Supplementary
288 Fig. 11). *D*-statistics (Fig. 4b,c) provided further support for excessive allele sharing between
289 the USA and Asia relative to that between the USA and other regions (Fig. 4b). This
290 admixture may reflect multiple waves of dispersal with canids across the Bering Land Bridge
291 in the Late Pleistocene during periods of ice sheet contraction [16] between 11–30 kya and
292 60–70 kya. Our population demographic data provide some support for this hypothesis, at
293 least during 11–30 kya, when USA and Asian populations experienced a close overlap in Ne
294 before undergoing rapid and distinct divergence thereafter (Figure 3b).

295

296 **The origin and spread of heartworms in Australia**

297 Heartworms are endemic in Australia, but the mechanisms and timing of their arrival in the
298 country have remained an enigma. Consistent with the modern human dispersal hypothesis,
299 one means of introduction could have been after European colonisation that began ~235
300 years ago. However, considering our genetic evidence of older, canid-mediated dispersal, a
301 more likely scenario is that heartworms were brought to Australia via dingos. The dingo, an
302 ancient lineage from Asia, was the only canid present on the Australian continent until
303 European settlement. Recent morphometric analysis indicates an East Asian origin of
304 dingoes via Melanesia [41], whereas genetic studies suggest that dingoes likely came from
305 Island Southeast Asia and were brought to Australia by humans between 5 and 12 kya[42].

306 Multiple lines of evidence support the introduction of heartworms into Australia via
307 Asia. Both admixture and TreeMix analyses highlighted the close relationship, evidenced by
308 partial or complete admixture profiles (Fig. 1e) and mutual monophyly (Fig. 4a) between
309 Asian samples and samples collected along the East Coast of Australia (Fig. 5a). Calculations
310 of D_{XY} showed that AUS-ASIA (D_{XY}[mean] = 5.13×10^{-4}) was the second least divergent pair
311 (after EUR-CENAM, which indicates a much more recent dispersal pattern; see below),
312 suggesting that Australian worms are more closely related to those in Asia than elsewhere
313 (Supplementary Fig. 10a). *D*-statistics solidified this relationship by showing excessive allele
314 sharing between the two continents relative to that between Australia and other regions
315 (Fig. 5b). These findings suggest an Asian origin of Australian heartworms, likely transported
316 with a dingo host, rather than through introduction by European colonisation. Finally,
317 samples from Australia and Asia exhibit very similar population demographic trajectories of
318 Ne until 10–20 kya, which begin to diverge in the post-domestication period, consistent with

319 the timing of the arrival of dingos rather than importation with European colonisation
320 (Figure 3c). We note that our sampling of Asian heartworms was from Thailand and
321 Peninsular Malaysia, which are geographically distinct from Indonesia, from which dogs
322 would have entered Australia from approximately 5 to 12 kya, potentially explaining the
323 small discrepancy in the estimated time of divergence. Sampling across a broader
324 geographic region, particularly throughout the Indonesian archipelago and Melanesia, could
325 bridge the gap between our Australian and Asian samples and provide further granularity of
326 the Asia–Australia divergence, potentially coinciding more closely with the timeline of dingo
327 arrival.

328 Considering the extensive sampling along the north–south transect of eastern
329 Australia, we sought to identify factors that might explain the current genetic diversity.
330 Australian heartworms were the second most genetically diverse population globally (Fig.
331 1c). Within Australia, diversity was highest in Lockhart River (Pi[mean] = 8.12×10^{-4}) and
332 lowest in Rockhampton (Pi[mean] = 2.15×10^{-4}) (Fig. 5c). Heartworms from the northern
333 state of Queensland were highly admixed, with two unique sources of ancestry not found on
334 any other continent (Fig. 1e). Interestingly, ten of 16 heartworms from Sydney, the
335 southernmost site, had a single fixed ancestry that was detected in Queensland samples.
336 Another four Sydney heartworms had a different fixed ancestry identical to that found in
337 Asia, potentially reflecting modern movement, though the exact cause remains unclear.
338 Previously, it was believed that heartworm cases in temperate Sydney and broader New
339 South Wales were primarily caused by infected pets or mosquitoes travelling down from
340 tropical and subtropical Queensland [43], where climates are more favourable to heartworm
341 transmission. However, our nuclear PCA showed a large cluster of samples primarily from
342 Queensland, alongside two distinct clusters from Sydney (Fig. 5d). This suggests that Sydney

343 heartworms may not necessarily originate from Queensland, as previously believed. Further
344 investigations are required to determine whether there are local endemic populations of
345 heartworms in Sydney. Differences in D_{XY} and F_{ST} between Australian heartworm
346 subpopulations were subtle, showing no clear relationship between genetic and
347 geographical distance as might be expected for a vector-borne parasite (Fig. 5e, f).

348

349 **Modern heartworm dispersal between Europe and Central America**

350 Our genomic analysis revealed a close genetic relationship between worms in Europe and
351 Central America. This finding was most evident in our PCA of nuclear SNPs, where samples
352 from Greece, Italy, and Romania clustered with those from Costa Rica and Panama (Fig. 1b).
353 In addition, estimates of D_{XY} revealed that EUR-CENAM (D_{XY}[mean] = 4.95×10^{-4}) was the
354 least divergent compared with other populations. Admixture analysis using NGSadmix
355 further supported this trend as the European and Central American samples shared high
356 levels of ancestry at lower *K* values (*K* = 2, 3, and 5; Supplementary Fig. 8). Although
357 increasing *K* helped to differentiate worms from these two continents, low levels of
358 admixture were still present (Fig. 1e). These findings were corroborated using *D*-statistics
359 which provided strong evidence of excessive allele sharing between heartworms from
360 Central America and Europe relative to that between Central America and other regions
361 (Fig. 4c). These findings support a modern migration event between European and Central
362 American heartworms which took place after dog domestication.

363 One plausible modern migration event between Europe and Central America was the
364 transatlantic transportation of domestic animals, including dogs, during the European
365 colonisation of the Americas, which began in the late 15th century. Animals introduced to

366 the Americas during the Age of Discovery were primarily livestock species, including cattle,
367 sheep, pigs, goats, horses, and mules. However, dogs such as greyhounds and mastiffs were
368 also introduced for hunting, guarding, protection, shepherding, and battle purposes [44–46].
369 The introduction of European dogs into the Americas is perhaps best documented from
370 Columbus' voyages, with historical records indicating the presence of at least 20 dogs on
371 board during the second voyage to Hispaniola [44]. Therefore, infected dogs from Europe may
372 have transported local strains of this parasite to the Americas. Alternatively, the shared
373 ancestry between European and Central American heartworms could result from the more
374 recent migration of humans and their pets. Although there is some variation in Ne between
375 EUR and CENAM over deeper evolutionary timescales, there is considerable overlap;
376 moreover, there is a striking divergence in Ne between populations around 500 years ago
377 (Figure 3d), consistent with our hypothesis that there is a recent connection between these
378 two populations over the past few centuries that have since diverged.

379

380 **Concluding remarks**

381 Our transcontinental genome-wide analysis of heartworm parasites has revealed a much
382 deeper origin and dispersal history than previously understood, allowing us to propose new
383 hypotheses on the evolutionary history of heartworms (Fig. 6). Rather than being solely
384 driven by human-mediated dispersal of dogs over the past few hundred years, we found
385 that ancestral canid hosts played a pivotal role in the evolution and dissemination of
386 heartworms around the world. Heartworms have evolved to exploit a unique niche in the
387 heart and bloodstream of canids, an environment that has likely remained unchanged over

388 millions of years between hosts. In the absence of niche competition, heartworms could be
389 a relic of the past, which, until recently, had little need for further adaptation.

390 Anthropogenic influence is, however, likely to shape heartworm diversity more
391 rapidly than ever before. For example, extensive drug treatment is already associated with
392 resistance, particularly in the USA; climate change is expected to shift populations of
393 parasites and their vectors into higher latitudes; and increasing global connectivity of people
394 and their pets will all influence the distribution and adaptation of heartworms. Therefore,
395 understanding the global genomic landscape of these parasites, as demonstrated here, is
396 vital for developing effective surveillance and control strategies in the future. Our data
397 indicate that such surveillance and control strategies should account for geographical
398 variation between parasite populations and be aware of transmission within and between
399 populations to maximise sustainable parasite control.

400

401 ## Methods

402 **Sample collection**

403 A total of 120 individual adult *Dirofilaria immitis* were obtained from Australia (*n* = 43), the
404 USA (*n* = 37), Panama (*n* = 14), Greece (*n* = 12), Thailand (*n* = 6), Italy (*n* = 3), Romania (*n* =
405 3), Costa Rica (*n* = 1), and Malaysia (*n* = 1). The sampling regime aimed to collect adult *D.*
406 *immitis* from a wide geographical range. Most of these samples were obtained from dogs
407 (*Canis lupus familiaris*; *n* = 115) but also included some from cats (*Felis catus*; *n* = 4), foxes
408 (*Vulpes vulpes*; *n* = 4), a ferret (*Mustela putorius furo*; *n* = 1), a golden jackal (*Canis aureus*; *n*
409 = 1), a leopard (*Panthera pardus*; *n* = 1), and a wildcat (*Felis silvestris*; *n* = 1) (metadata for all

410 samples is presented in Supplementary Data 2). We included five technical replicates
411 (Brisbane: *n* = 1; Sydney: *n* = 2; Malaysia: *n* = 1; Panama: *n* = 1). To provide outgroup
412 samples for our analyses, we collected adult *D. repens* (*n* = 2) from dogs in Italy, *Dirofilaria*
413 sp. 'Thailand II' (*n* = 2) from humans (*Homo sapiens*) in Vietnam and *D. ursi* (*n* = 1) from an
414 American black bear (*Ursus americanus*) in the USA (Supplementary Data 1).

415

416 **DNA extraction and whole genome sequencing**

417 *Dirofilaria* specimens were frozen at −20°C or stored in ethanol upon collection and sent to
418 the University of Sydney, Australia. A 1–2 cm segment between the first and second third of
419 the anterior portion of the worms was excised using a sterile scalpel blade and placed in a
420 1.5 mL Eppendorf tube.

421 ***Ethanol-preserved samples.*** Worm segments were centrifuged at maximum speed
422 for 30 s using a benchtop centrifuge (Eppendorf, Australia) and excess ethanol was
423 removed. The segments were washed in 500 mL of phosphate-buffered saline (PBS) and
424 placed on a heat block (Heat Block Eppendorf Thermomixer Comfort or Heat Block Major
425 Science Dry Bath Incubator) at 60°C for 20–40 min, depending on their thickness, to
426 evaporate any remaining ethanol.

427 ***Frozen samples.*** Worm segments were defrosted and washed three times in PBS.
428 Genomic DNA was extracted from the tissue segments using a Monarch® Genomic DNA
429 Purification Kit (New England Biolabs, Australia) as per the manufacturer's protocol.
430 Extracted DNA was shipped to Novogene (HK) Co., Ltd for indexing, library preparation, and

431 whole genome sequencing using the NovaSeq 6000 platform. Overall, 128/130 and 2/130
432 DNA samples were sequenced at expected depths of ~10 G and ~1 G, respectively.

433

434 **Bioinformatic analyses**

435 The bioinformatics workflow of this study is summarised in Supplementary Fig. 12. In
436 addition to the data generated in this study, we included publicly available datasets of
437 individual *D. immitis*. These data were derived from (i) five adults from Sydney, Australia
438 (SRA NCBI: SRR13154013-7) [47]; (ii) one adult from Georgia, USA (ENA Accession: ERR034940)
439 and one adult from Pavia, Italy (ENA Accession: ERR034941) [48].

440

441 **Raw data processing and mapping**

442 Multiple FastQ files were generated for some samples and merged before data analysis. The
443 quality of all raw paired-end sequencing reads was inspected using FastQC (version 0.11.8;
444 https://www.bioinformatics.babraham.ac.uk/projects/fastqc/), and the output was
445 summarised using MultiQC (version 1.17 [49]). The raw paired-end reads were scanned with a
446 10-base sliding window and trimmed to have a minimum average quality score of 20 per
447 base and a minimum read length of 50 bp using Trimmomatic [50] (version 0.39). We used a
448 Nextflow [51] mapping pipeline (mapping-helminth/v1.0.9 [52]) to map the trimmed paired-end
449 reads to a combined reference genome containing *D. immitis* (dimmitis_WSI_2.2 [25]) and the
450 domestic dog (GenBank accession: GCA_014441545). The dimmitis_WSI_2.2 genome has
451 been previously supplemented with the *D. immitis* mitochondrial and *D. immitis*-associated
452 *Wolbachia* endosymbiont genomes [25]. The mapping pipeline was designed for the standard

453 mapping of helminth genomes using Minimap2 (version 2.17 [53]) as a mapper and GATK
454 (version 4.1.4.1 [54]), Samtools (version 1.14 [55]), and Sambamba (version 1.0 [56]) for further
455 data processing. Reads aligning to only the *D. immitis* genome were extracted for
456 downstream analysis using Samtools.

457

458 **Sequencing Coverage**

459 Sequencing coverage was examined using BamTools (version 2.5.1 [57]), BEDTools
460 makewindows (version 2.31.0 [58]), and SAMtools bedcov. Coverage statistics were obtained
461 for the nuclear, mitochondrial, and *Wolbachia* genomes of *D. immitis*. To visualise nuclear *D.*
462 *immitis* sequencing coverage for each sample, the scaffold, mitochondrial and *Wolbachia*
463 genomes of *D. immitis* were removed, along with any chromosomes of the domestic dog
464 genome. The ratio of X chromosome to autosome coverage was visualised to determine the
465 sex of the *D. immitis* samples, identified by a drop in coverage along the X chromosome
466 (ratio ~ 0.5) indicative of a male parasite [25].

467

468 **Variant calling**

469 Variants were identified using GATK (version 4.1.4.1; [54]) HaplotypeCaller, CombineGVCFs,
470 and GenotypeGVCFs. GVCF files were first produced for each sample and then combined
471 into a cohort-level GVCF file, which was then used for joint genotyping. Outgroup samples
472 were removed to obtain a *D. immitis* cohort VCF file. Variants in the nuclear, mitochondrial,
473 and *Wolbachia* datasets were filtered separately using GATK SelectVariants, GATK
474 VariantFiltration, and VCFtools (version 1.16 [59]). The distribution of eight quality metrics was

475 established (QUAL, DP, MQ, SOR, QD, FS, MQRankSum, and ReadPosRankSum), and the
476 relevant upper and/or lower 1% distribution tails were removed. The single nucleotide
477 variants (SNVs) were further filtered based on the following parameters: bi-allelic, depth ≥3,
478 Hardy-Weinberg Equilibrium p-value $\geq 10^{-6}$ (nuclear), and minor allele frequency ≥0.02.
479 Indels were not included in subsequent analyses. Samples with <50% of the total variants
480 were removed, and an optimal threshold for missing data of 0.9 was established (nuclear,
481 mitochondrial, and *Wolbachia*). Additional VCF files were generated from the filtered
482 nuclear data for autosomes (chromosomes 1–4), the sex-linked X chromosome, and
483 Australian samples. The same filtering parameters were applied to the VCF file containing
484 both *D. immitis* and outgroup samples. SNP discordance in the filtered nuclear autosome
485 data for the technical replicate samples was measured using VCFtools --diff-indv-
486 discordance. All technical replicates had <0.5% SNP discordance with their respective
487 original samples.

488

489 **Population structure**

490 To explore the broad-scale genetic relatedness between *D. immitis* individuals and
491 populations, we performed principal component analysis (PCA) using the R package
492 SNPRelate (version 1.38.0; [60]). PCA was conducted for the nuclear (autosomes together,
493 autosomes separate, and chromosome X separate), mitochondrial, and *Wolbachia* data.

494 Nucleotide diversity (Pi) within populations, as well as absolute nucleotide
495 divergence (D_{XY}) and genetic differentiation (F_{ST}) between populations, were calculated
496 using pixy (version 1.2.10.beta2; [61]). First, the GVCF files were genotyped using GATK
497 GenotypeGVCFs with the inclusion of invariant sites (--all-sites). The nuclear invariants were

498 selected using GATK SelectVariants (--select-type-to-include NO_VARIATION) and merged
499 with the previously filtered nuclear SNPs. The VCF file was filtered to only include invariants
500 and SNPs in the autosomes and sex-linked X chromosome. We conducted the pixy analysis
501 with a window size of 100 kb. Separate runs were performed, grouping the samples in
502 various ways: by region (using dog host samples only), by host species (using all samples),
503 and by city/state (using Australian dog host samples only).

504 Linkage disequilibrium (LD) statistics were obtained from the nuclear data using
505 VCFtools. First, we filtered and thinned the data (--maf 0.02 --thin 1000 --max-missing 1).
506 We then calculated the squared correlation coefficient between genotypes (--ld-window-bp
507 1000000 --max-alleles 2 --min-alleles 2 --min-r2 0.1 --geno-r2). To visualise patterns of LD
508 decay, the output was plotted per 0.1 kb for each population.

509

510 **Admixture**

511 The global ancestry and admixture proportions of *D. immitis* were inferred using NGSadmix
512 from the ANGSD package [62]. First, genotype likelihoods were extracted from the filtered
513 autosomal *D. immitis* VCF file using VCFtools (--max-missing 1 --BEAGLE-PL). Genotype
514 likelihoods were extracted separately for each chromosome and merged into a single
515 dataset. NGSadmix (-minMaf 0.02 -misTol 0.9) was performed using multiple combinations
516 of different clusters (*K* = 2 to 10) and seeds (1 to 5). CLUMPAK was used to determine the
517 optimal *K* value [63].

518 We used TreeMix (version 1.12; [64]) to produce a maximum-likelihood tree and infer
519 population splits and admixture events in the *D. immitis* dataset. To generate the input data,

520 VCFtools was used to filter the cohort SNV VCF file (--max-missing 1), retaining only
521 autosomal data and the same samples as in the previous variant-calling filtration step. The
522 variants were pruned for linkage disequilibrium (10 kb windows, shifting by 10 kb, LD
523 threshold 0.1), and the VCF file was converted to the appropriate format using custom
524 scripts ('ldPruning.sh' and 'vcf2treemix.sh') obtained from
525 https://github.com/speciationgenomics/scripts. TreeMix was run across a range of
526 migration edges (0 to 5) and seeds (0 to 10), with *D. ursi* included as an outgroup. The
527 optimal number of migration edges was estimated using the R package OptM (version 1.8;
528 https://github.com/cran/OptM).

529 To further investigate admixture in the cohort, *D*-statistics were inferred using
530 AdmixTools (version 5.1 [65]). First, we converted our filtered nuclear VCF file into the
531 required eigenstrat format using a custom script ('convertVCFtoEigenstrat.sh') obtained
532 from https://github.com/speciationgenomics/scripts/. Additional tools required for file
533 conversion were VCFtools and PLINK (version 1.90b6.18 [66]). qpDstat was used to perform *D*-
534 statistic testing for all population pairs relative to the other populations (PopX), with *D. ursi*
535 as the outgroup taxa. *Z*-scores with an absolute value >3 were considered significant.

536

537 **Population demography**

538 We estimated the population size history of *D. immitis* using SMC++[71] (version 1.15.4 [67]).
539 Samples from dog hosts in the filtered autosomal VCF were grouped by continent (*i.e.*, Asia,
540 Australia, Central America, Europe, and USA) and analysed separately before being plotted
541 together. First, a mask of the genome was performed to exclude non-variable sites, using
542 *bcftools query* of the VCF to generate a bed file of variable positions and then *bcftools*

543 *subtract* using a bed file of the genome to identify genomic positions not found in the VCF.
544 Per population, vcftools was used to extract population-specific variants from the autosomal
545 VCF file (--keep <POP>), ensuring no missing sites (--max-missing 1) and no HWE filter
546 applied. Then, the filtered VCF file was converted to the SMC++ input format using *smc++*
547 *vcf2smc* (including --mask missing_sites.bed.gz). *vcf2smc* was run on each chromosome
548 individually (n = 4 autosomes), before a combined model was was fitted using *smc++*
549 *estimate* with a timepoint range of 1 to 1,000,000 and the nematode *Caenorhabditis*
550 *elegans* mutation rate of 2.7×10^{-9} per site per generation as a proxy for the *D. immitis*
551 mutation rate, which is currently unknown. We acknowledge that without a specific *D.*
552 *immitis* mutation rate, there will be some uncertainty in the population demographic
553 models and that Ne at specific times may be over or underestimated; however, very few
554 mutation rates have been determined for nematodes [68], and previous studies on parasitic
555 worms have used the *C. elegans* rate as a default [20,21,69,70]. To understand the variance in the
556 model output, we also iteratively ran *smc++ vcf2smc* and *smc++ estimate,* but excluded one
557 chromosome at a time, which allowed us to generate a confidence interval around the "all
558 chromosome" model. To visualise the models, the *smc++ plot* command (-g -c) was used,
559 with the -g parameter specifying the generation time of the target population. The
560 generation time of *D. immitis* is not precisely known, but is estimated to take up to one year
561 to produce offspring from an established infection. However, infections are rarely found in
562 hosts <1 year old, and the adult worms can live for up to 7 years in the host's
563 cardiopulmonary system. Furthermore, the development and transmission of this parasite
564 are also highly dependent on local climate and the availability of vectors. To account for
565 potential variability in the generation time of *D. immitis*, we tested multiple generation

566 times (-g 1, 2.5, or 4) (Supplementary Fig. 13), settling on a midpoint of 2.5 years for major
567 comparisons.

568

569 Data availability

570 Raw FastQ sequences generated in this study are available at SRA NCBI BioProject
571 PRJNA1104412.

572

573 Code availability

574 The code used to analyse the data in this study is available from GitHub:
575 https://github.com/rosemondepower/heartworm_genome.git.

576 ## References

577 1. Noack, S., Harrington, J., Carithers, D. S., Kaminsky, R. & Selzer, P. M. Heartworm
578 disease - Overview, intervention, and industry perspective. *Int. J. Parasitol. Drugs Drug*
579 *Resist.* **16**, 65–89 (2021).
580 2. Bowman, D. D. & Atkins, C. E. Heartworm biology, treatment, and control. *Vet. Clin.*
581 *North Am. Small Anim. Pract.* **39**, 1127–58, vii (2009).
582 3. Nelson, T., McCall, J. W., Moorhead, A., Starkey, L. & Ames, M. *American Heartworm*
583 *Society Canine Guidelines for the Prevention, Diagnosis, and Management of*
584 *Heartworm (Dirofilaria Immitis) Infection in Dogs*.
585 https://d3ft8sckhnqim2.cloudfront.net/images/AHS_Canine_Guidelinesweb22NOV202
586 4.pdf?1732318144 (2024).
587 4. Hampshire, V. A. Evaluation of efficacy of heartworm preventive products at the FDA.
588 *Vet Parasitol* **133**, 191–195 (2005).
589 5. Pulaski, C. N. *et al.* Establishment of macrocyclic lactone resistant *Dirofilaria immitis*
590 isolates in experimentally infected laboratory dogs. *Parasit. Vectors* **7**, 494 (2014).
591 6. Simón, F. *et al.* Human and animal dirofilariasis: the emergence of a zoonotic mosaic.
592 *Clin. Microbiol. Rev.* **25**, 507–544 (2012).
593 7. Roncalli, R. Tracing the history of heartworms: A 400 year perspective. in *Recent*
594 *Advances in Heartworm Disease: AHS Symposium* (1998). doi:10.5555/20053201369.
595 8. Belanger, D. H., Perkins, S. L. & Rockwell, R. F. Inference of population structure and
596 patterns of gene flow in canine heartworm (*Dirofilaria immitis*). *J. Parasitol.* **97**, 602–
597 609 (2011).
598 9. Sanchez, J. *et al.* Using population genetics to examine relationships of *Dirofilaria*

599 *immitis* based on both macrocyclic lactone-resistance status and geography. *Vet*
600 *Parasitol* **283**, 109125 (2020).
601 10. Morchón, R. *et al.* New insights into the phylogeographic history of *Dirofilaria immitis*
602 in the Canary Islands, Spain. *Animals* **15**, 1694 (2025).
603 11. Alsarraf, M. *et al.* Diversity and geographic distribution of haplotypes of *Dirofilaria*
604 *immitis* across European endemic countries. *Parasites & Vectors* **16**, 1–12 (2023).
605 12. Moroni, B. *et al. Dirofilaria immitis* in wolves recolonizing northern Italy: are wolves
606 competent hosts? *Parasit. Vectors* **13**, 482 (2020).
607 13. Aher, A. M. *et al.* Prevalence, genetic analyses, and risk factors associated with
608 heartworm (*Dirofilaria immitis*) in wild coyotes (*Canis latrans*) from Florida, USA. *J.*
609 *Wildl. Dis.* **52**, 785–792 (2016).
610 14. Wang, X. & Tedford, R. H. *Dogs: Their Fossil Relatives and Evolutionary History*.
611 (Columbia University Press, New York, NY, 2010).
612 15. Villmoare, B. *et al.* Paleoanthropology. Early *Homo* at 2.8 Ma from Ledi-Geraru, afar,
613 Ethiopia. *Science* **347**, 1352–1355 (2015).
614 16. Bergström, A. *et al.* Grey wolf genomic history reveals a dual ancestry of dogs. *Nature*
615 **607**, 313–320 (2022).
616 17. Freedman, A. H. *et al.* Genome sequencing highlights the dynamic early history of dogs.
617 *PLoS Genet.* **10**, e1004016 (2014).
618 18. Botigué, L. R. *et al.* Ancient European dog genomes reveal continuity since the Early
619 Neolithic. *Nat. Commun.* **8**, 16082 (2017).
620 19. Soghigian, J. *et al.* Phylogenomics reveals the history of host use in mosquitoes. *Nat.*
621 *Commun.* **14**, 6252 (2023).
622 20. Sallé, G. *et al.* The global diversity of *Haemonchus contortus* is shaped by human

623 intervention and climate. *Nat. Commun.* **10**, 4811 (2019).

624 21. Doyle, S. R. *et al.* Population genomics of ancient and modern *Trichuris trichiura*. *Nat.*
625 *Commun.* **13**, 3888 (2022).

626 22. Small, S. T. *et al.* Human migration and the spread of the nematode parasite
627 *Wuchereria bancrofti*. *Mol. Biol. Evol.* **36**, 1931–1941 (2019).

628 23. Power, R. I., Doyle, S. R. & Šlapeta, J. Whole genome amplification and sequencing of
629 individual *Dirofilaria immitis* microfilariae. *Exp. Parasitol.* **263-264**, 108806 (2024).

630 24. Choi, Y.-J. *et al.* Genomic diversity in *Onchocerca volvulus* and its *Wolbachia*
631 endosymbiont. *Nat Microbiol* **2**, 16207 (2016).

632 25. Gandasegui, J. *et al.* Genome structure and population genomics of the canine
633 heartworm *Dirofilaria immitis*. *Int. J. Parasitol.* (2023) doi:10.1016/j.ijpara.2023.07.006.

634 26. Atkinson, P. J., Stevenson, M., O'Handley, R., Nielsen, T. & Caraguel, C. G. B.
635 Temperature-bounded development of *Dirofilaria immitis* larvae restricts the
636 geographical distribution and seasonality of its transmission: case study and decision
637 support system for canine heartworm management in Australia. *Int. J. Parasitol.* **54**,
638 311–319 (2024).

639 27. Penezić, A., Selaković, S., Pavlović, I. & Ćirović, D. First findings and prevalence of adult
640 heartworms (*Dirofilaria immitis*) in wild carnivores from Serbia. *Parasitol. Res.* **113**,
641 3281–3285 (2014).

642 28. Ionică, A. M., Deak, G., Boncea, R., Gherman, C. M. & Mihalca, A. D. The European
643 badger as a new host for *Dirofilaria immitis* and an update on the distribution of the
644 heartworm in wild carnivores from Romania. *Pathogens* **11**, 420 (2022).

645 29. McCall, J. W., Genchi, C., Kramer, L. H., Guerrero, J. & Venco, L. Heartworm disease in
646 animals and humans. *Adv. Parasitol.* **66**, 193–285 (2008).

30. Molnár, V. *et al.* Autochthonous *Dirofilaria immitis* infection in a ferret with aberrant larval migration in Europe. *J. Small Anim. Pract.* **51**, 393–396 (2010).

31. vonHoldt, B. M. *et al.* Whole-genome sequence analysis shows that two endemic species of North American wolf are admixtures of the coyote and gray wolf. *Sci. Adv.* **2**, e1501714 (2016).

32. Small, S. T., Tisch, D. J. & Zimmerman, P. A. Molecular epidemiology, phylogeny and evolution of the filarial nematode *Wuchereria bancrofti*. *Infect. Genet. Evol.* **28**, 33–43 (2014).

33. Chavez, D. E. *et al.* Comparative genomics uncovers the evolutionary history, demography, and molecular adaptations of South American canids. *Proc. Natl. Acad. Sci. U. S. A.* **119**, e2205986119 (2022).

34. Leonard, J. A. *et al.* Megafaunal extinctions and the disappearance of a specialized wolf ecomorph. *Curr. Biol.* **17**, 1146–1150 (2007).

35. Hofreiter, M. Pleistocene extinctions: haunting the survivors. *Curr. Biol.* **17**, R609–11 (2007).

36. Jiangzuo, Q. *et al.* Middle Pleistocene *Xenocyon lycaonoides* Kretzoi, 1938 in northeastern China and the evolution of Xenocyon-Lycaon lineage. *Hist. Biol.* 8912963.2021.2022138 (2022).

37. Rook, L. The wide ranging genus *Eucyon* Tedford & Qiu, 1996 (Mammalia, Carnivora, Canidae, Canini) in the Mio-Pliocene of the Old World. *Geodiversitas* **31**, 723–741 (2009).

38. Kukla, G. J. *et al.* Last interglacial climates. *Quat. Res.* **58**, 2–13 (2002).

39. Batchelor, C. L. *et al.* The configuration of Northern Hemisphere ice sheets through the Quaternary. *Nat. Commun.* **10**, 3713 (2019).

671 40. Koblmüller, S. *et al.* Whole mitochondrial genomes illuminate ancient intercontinental
672 dispersals of grey wolves (*Canis lupus*). *J. Biogeogr.* **43**, 1728–1738 (2016).
673 41. Koungoulos, L. G., Hulme-Beaman, A., Fillios, M. & Willandra Lakes Region World
674 Heritage Aboriginal Advisory Group. Phenotypic diversity in early Australian dingoes
675 revealed by traditional and 3D geometric morphometric analysis. *Sci. Rep.* **14**, 21228
676 (2024).
677 42. Fillios, M. A. & Taçon, P. S. C. Who let the dogs in? A review of the recent genetic
678 evidence for the introduction of the dingo to Australia and implications for the
679 movement of people. *J. Archaeol. Sci. Rep.* **7**, 782–792 (2016).
680 43. McKeever, B., Podadera, J. M., Beijerink, N. J. & Šlapeta, J. Suspect 'baggage canine
681 heartworm' case: canine heartworm disease in a dog from Sydney, New South Wales.
682 *Aust. Vet. J.* **99**, 359–362 (2021).
683 44. Ensminger, J. J. From hunters to hell hounds: the dogs of Columbus and
684 transformations of the human-canine relationship in the early Spanish Caribbean.
685 *Colon. Latin Am. Rev.* **31**, 354–380 (2022).
686 45. Symcox, G. & Sullivan, B. Introduction: Columbus—the man, the voyages, the legacy. in
687 *Christopher Columbus and the Enterprise of the Indies* 1–40 (Palgrave Macmillan US,
688 New York, 2005).
689 46. Welker, M. H. & Dunham, R. Exploring the introduction of European dogs to North
690 America through shoulder height. *Int. J. Osteoarchaeol.* **29**, 325–334 (2019).
691 47. Lau, D. C.-W. *et al.* Whole-genome reference of from Australia to determine single
692 nucleotide polymorphisms associated with macrocyclic lactone resistance in the USA.
693 *Curr. Res. Parasitol. Vector Borne Dis*. **1**, 100007 (2021).
694 48. Godel, C. *et al.* The genome of the heartworm, *Dirofilaria immitis*, reveals drug and

695 vaccine targets. *FASEB J.* **26**, 4650–4661 (2012).

696 49. Ewels, P., Magnusson, M., Lundin, S. & Käller, M. MultiQC: summarize analysis results
697 for multiple tools and samples in a single report. *Bioinformatics* **32**, 3047–3048 (2016).

698 50. Bolger, A. M., Lohse, M. & Usadel, B. Trimmomatic: a flexible trimmer for Illumina
699 sequence data. *Bioinformatics* **30**, 2114–2120 (2014).

700 51. Di Tommaso, P. *et al.* Nextflow enables reproducible computational workflows. *Nat.*
701 *Biotechnol.* **35**, 316–319 (2017).

702 52. McIntyre, J. *et al.* Chromosomal genome assembly resolves drug resistance loci in the
703 parasitic nematode *Teladorsagia circumcincta*. *PLoS Pathog*. **21**, e1012820 (2025).

704 53. Li, H. Minimap2: pairwise alignment for nucleotide sequences. *Bioinformatics* **34**,
705 3094–3100 (2018).

706 54. Van der Auwera, G. A. & O'Connor, B. D. *Genomics in the Cloud: Using Docker, GATK,*
707 *and WDL in Terra*. (O'Reilly Media, 2020).

708 55. Danecek, P. *et al.* Twelve years of SAMtools and BCFtools. *Gigascience* **10**, giab008
709 (2021).

710 56. Tarasov, A., Vilella, A. J., Cuppen, E., Nijman, I. J. & Prins, P. Sambamba: fast processing
711 of NGS alignment formats. *Bioinformatics* **31**, 2032–2034 (2015).

712 57. Barnett, D. W., Garrison, E. K., Quinlan, A. R., Strömberg, M. P. & Marth, G. T.
713 BamTools: a C++ API and toolkit for analyzing and managing BAM files. *Bioinformatics*
714 **27**, 1691–1692 (2011).

715 58. Quinlan, A. R. & Hall, I. M. BEDTools: a flexible suite of utilities for comparing genomic
716 features. *Bioinformatics* **26**, 841–842 (2010).

717 59. Danecek, P. *et al.* The variant call format and VCFtools. *Bioinformatics* **27**, 2156–2158
718 (2011).

719 60. Zheng, X. *et al.* A high-performance computing toolset for relatedness and principal
720 component analysis of SNP data. *Bioinformatics* **28**, 3326–3328 (2012).
721 61. Korunes, K. L. & Samuk, K. pixy: Unbiased estimation of nucleotide diversity and
722 divergence in the presence of missing data. *Mol. Ecol. Resour.* **21**, 1359–1368 (2021).
723 62. Skotte, L., Korneliussen, T. S. & Albrechtsen, A. Estimating individual admixture
724 proportions from next generation sequencing data. *Genetics* **195**, 693–702 (2013).
725 63. Kopelman, N. M., Mayzel, J., Jakobsson, M., Rosenberg, N. A. & Mayrose, I. Clumpak: a
726 program for identifying clustering modes and packaging population structure
727 inferences across K. *Mol. Ecol. Resour.* **15**, 1179–1191 (2015).
728 64. Pickrell, J. K. & Pritchard, J. K. Inference of population splits and mixtures from
729 genome-wide allele frequency data. *PLoS Genet.* **8**, e1002967 (2012).
730 65. Patterson, N. *et al.* Ancient admixture in human history. *Genetics* **192**, 1065–1093
731 (2012).
732 66. Chang, C. C. *et al.* Second-generation PLINK: rising to the challenge of larger and richer
733 datasets. *Gigascience* **4**, 7 (2015).
734 67. Terhorst, J., Kamm, J. A. & Song, Y. S. Robust and scalable inference of population
735 history from hundreds of unphased whole genomes. *Nat. Genet.* **49**, 303–309 (2017).
736 68. Wang, Y. & Obbard, D. J. Experimental estimates of germline mutation rate in
737 eukaryotes: a phylogenetic meta-analysis. *Evol Lett* **7**, 216–226 (2023).
738 69. Cole, R., Holroyd, N., Tracey, A., Berriman, M. & Viney, M. The parasitic nematode
739 *Strongyloides ratti* exists predominantly as populations of long-lived asexual lineages.
740 *Nat. Commun*. **14**, 6427 (2023).
741 70. Stevens, L. *et al.* Ancient diversity in host-parasite interaction genes in a model
742 parasitic nematode. *Nat. Commun.* **14**, 7776 (2023).

Acknowledgements

The authors gratefully acknowledge Julie Austin, Iris Cheadle, Constantin Constantinoiu, Carol Esson, Eloise Fenton, Linda Hayes, Tessa Mackie, Yissu Martinez, Sandi McClintock, Ilze Nel, Tony Phillis, Duncan Smith, and Jim Taylor for their generous provision of heartworm specimens for this study. Sampling from the University of Queensland was supported by the University of Queensland, School of Veterinary Science Bequest and Donation Funds for Research (Stone Memorial Fund). We thank Javier Gandasegui for their foundational bioinformatics work that facilitated this work. We acknowledge the Pathogen Informatics group at the Wellcome Sanger Institute and the Sydney Informatics Hub for bioinformatics support. RIP is supported by an Australian Government Research Training Program Stipend and The Jean Walker Trust Fellowship. RIP's collaborative research exchange was supported by the University of Sydney's Eric Horatio Scholarship, the University of Sydney's Postgraduate Research Support Scheme, and the Australian Society for Parasitology's Researcher Exchange, Training and Travel Award. SRD is supported by a UKRI Future Leaders Fellowship [MR/T020733/1] and the Wellcome Trust (UK) through core funding to the Wellcome Sanger Institute (UK) [206194]. This work was funded by the Canine Research Foundation, Dogs Victoria, Australia and the Australian Companion Animal Health Foundation Research Grant. For the purpose of Open Access, the authors have applied a CC BY public copyright Licence to any Author Accepted Manuscript version arising from this submission.

Author contributions

RIP and JŠ conceived and designed the study; JŠ and SRD co-supervised the study; SA, HSW, GGV, TLS, JLL, ARM, MTD, JMF, MLM, AR, SCC, GD, ADM, PD, EP, PT, DTB, ADN, RSKS, and JS provided materials; RIP extracted DNA and prepared samples for sequencing; RIP and SRD led and performed the bioinformatics analyses; RIP and SRD analysed and interpreted the results, with input from contributions from JŠ and SYWH; RIP drafted the original manuscript, with contributions from SRD and JŠ. All authors contributed to the revision and approved of the final manuscript.

Competing Interests

The authors declare no competing interests.

Figures

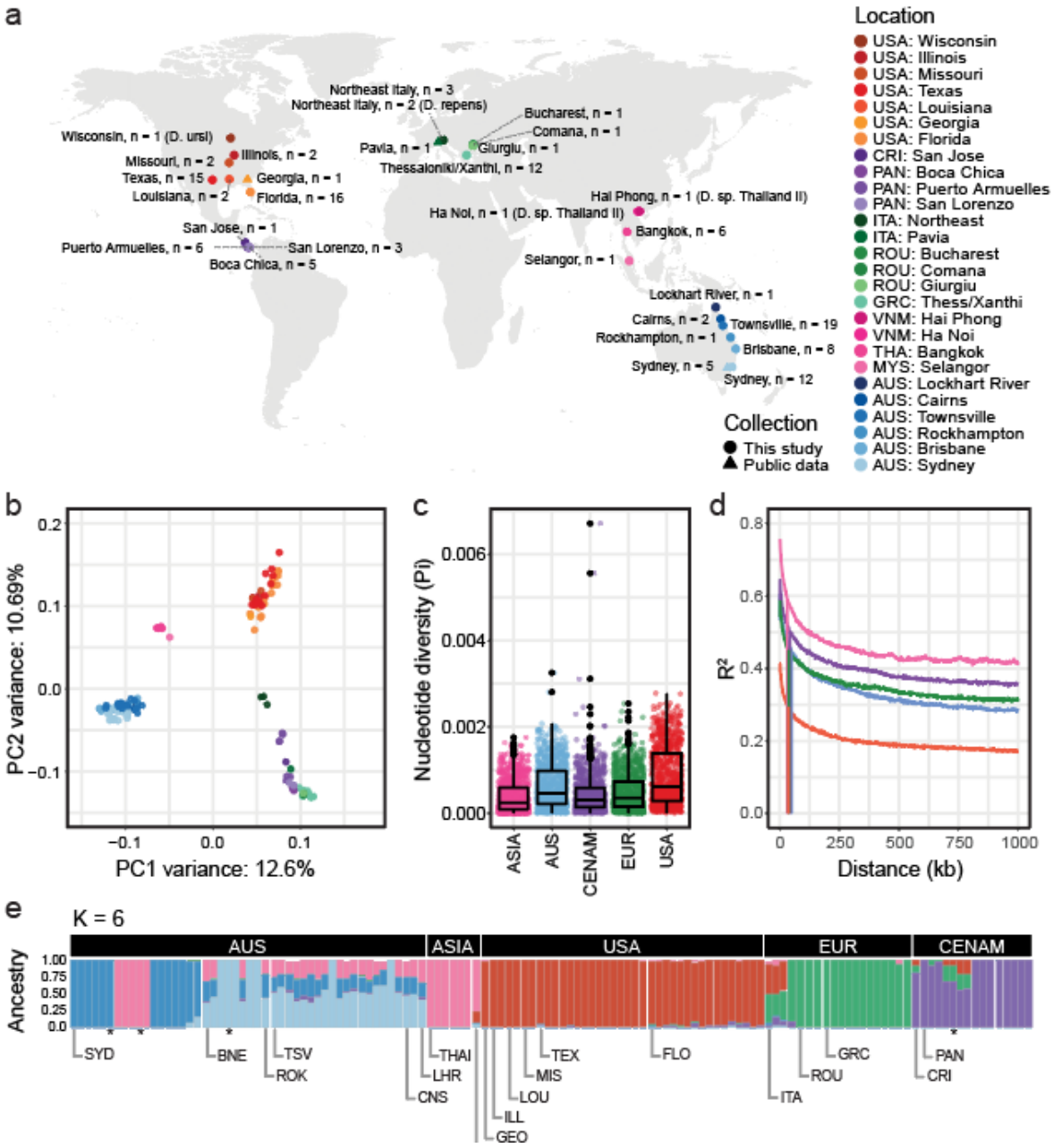

Fig. 1: Global sampling and population structure of heartworms. a, World map showing the location of adult heartworm specimens used in the study. Adult *Dirofilaria ursi*, *D. repens*, and *D*. sp. 'Thailand II' were included as outgroup samples. **b,** Principal component analysis (PCA) of 196,550 nuclear single nucleotide polymorphisms (SNPs) from 124 heartworms. **c,** Box plots showing the nucleotide diversity (Pi) distribution within broad geographical

783 regions, with each point representing a 100 kb sliding window. **d,** Linkage disequilibrium
784 (LD) decay plot for the heartworm cohort, grouped by broad geographic region. Vertical
785 lines show the distance between SNPs where the LD is half the maximum value. **e,**
786 Admixture inferred using NGSadmix with six clusters (K). Each vertical bar represents an
787 individual sample, with colours representing the clusters. Labels at the top of the bar charts
788 indicate the broad geographic origins of samples, while those at the bottom show their
789 more specific locations. An asterisk (*) denotes a replicate of the preceding sample.
790 Abbreviations: USA = United States of America (Georgia: GEO, Illinois: ILL, Louisiana: LOU,
791 Missouri: MIS, Texas: TEX, Florida: FLO); CRI = Costa Rica; PAN = Panama; ITA = Italy; ROU =
792 Romania; GRC = Greece; VNM = Vietnam; THA = Thailand; MYS = Malaysia; AUS = Australia
793 (Sydney: SYD, Brisbane: BNE, Rockhampton: ROK, Townsville: TSV, Cairns: CNS, Lockhart
794 River: LHR).

795

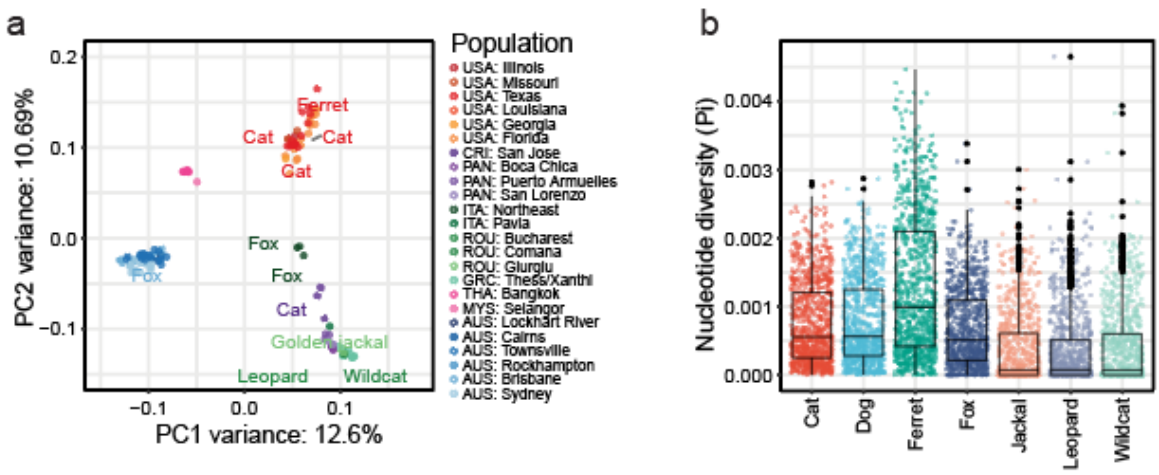

Fig. 2: Variation in the genetics and competency between heartworm hosts. a, Principal component analysis (PCA) of heartworm nuclear diversity from Fig. 1b, with non-dog hosts labelled. The geographic origin of samples is indicated on the right (i.e. COUNTRY: city or region). Country abbreviations: USA = United States of America; CRI = Costa Rica; PAN = Panama; ITA = Italy; ROU = Romania; GRC = Greece; VNM = Vietnam; THA = Thailand; MYS = Malaysia; AUS = Australia. **b,** Box plots show the distribution of nucleotide diversity (Pi) within host populations. Each data point represents a sliding window size of 100 kb. **c,** Support for the heartworm life cycle and adult worm burdens in carnivoran hosts. The top panel highlights hosts that are frequently microfilaremic and are hence considered competent reservoirs for heartworms. A black star indicates cases where microfilaremia has been reported in the host, but they are generally considered to pose a low risk of being competent reservoirs. The bottom panel is a plot showing adult heartworm burdens across various hosts. Each point represents data from a study, sourced from the literature (Supplementary Table 1). Significant differences in worm burdens among competent reservoirs were assessed using a Kruskal-Wallis test with Dunn's multiple comparisons. *P*-values ≤ 0.05 were considered statistically significant (*: ≤ 0.05, **: ≤ 0.01, ***: ≤ 0.001).

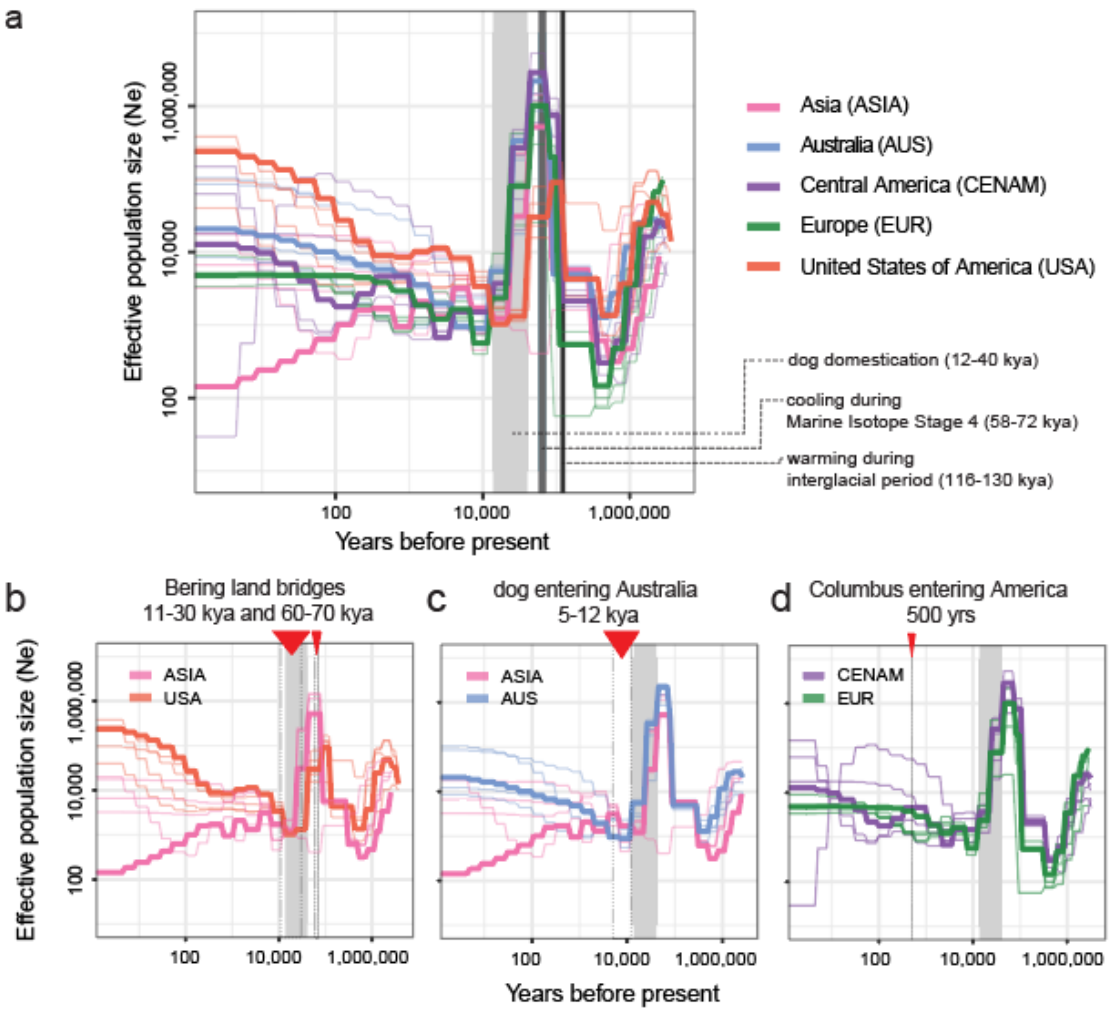

Fig. 3: Demographic history and host competency for heartworms. a, Effective population size history of heartworm populations inferred using SMC++ based on a 2.5-year generation time. Each thick line represents the effective population size of heartworms on each continent over time. Thin lines represent jackknife sampling of chromosomes, iteratively removing one of four autosomal chromosomes, to visualise variance in Ne. The light grey box spans ~14–40 kya, highlighting the previously suggested period of dog domestication, as well as dark grey boxes highlighting global cooling (58–72 kya) and warming (116–130 kya) periods. **b,c,d,** Reconfigured datasets from **a,** highlighting key pairwise comparisons to explore hypotheses presented in the text. **b,** Comparison of the effective population size histories of heartworm populations from Asia and the USA. The red arrows and dotted lines

represent periods of Bering land bridge exposure. **c,** Comparison of effective population size histories of Asian and Australian heartworm populations. The red arrow and dotted lines indicate the suggested period of dingo introduction in Australia. **d,** Comparison of effective population size histories of Central American and European heartworm populations. The red arrow with a dotted line indicates the period of European colonisation of the Americas. Abbreviations: AUS = Australia; CENAM = Central America; EUR = Europe; USA = United States of America.

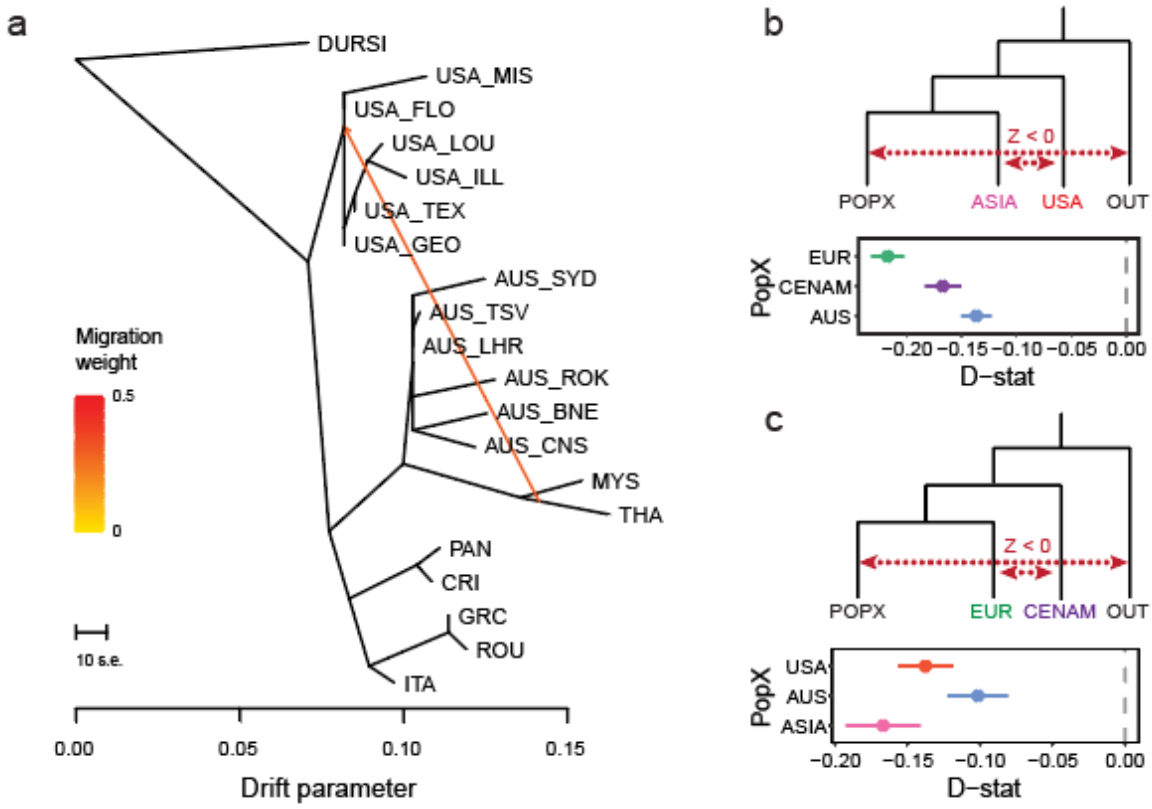

Fig. 4: Transcontinental admixture in heartworms. a, Maximum-likelihood tree of heartworm generated using TreeMix, with *Dirofilaria ursi* (DURSI) as an outgroup and one migration edge. **b,c,** *D*-statistics for hypothetical allele-sharing scenarios between heartworm populations using Admixtools qpDstat with 21,088 single nucleotide polymorphisms (SNPs) and *D. ursi* as the outgroup (OUT). *D*-statistics test for admixture between four populations (W, X, Y, Z). A Z-score (*D*-statistic / standard error) is calculated, which provides information about the direction of gene flow (red dotted lines) (Z-score > 0 = gene flow between either [W and Y], or [X and Z]; Z-score < 0 = gene flow between either [W and Z] or [X and Y]). For all data presented, the Z score was significant (|Z| > 3). Error bars show the standard error.

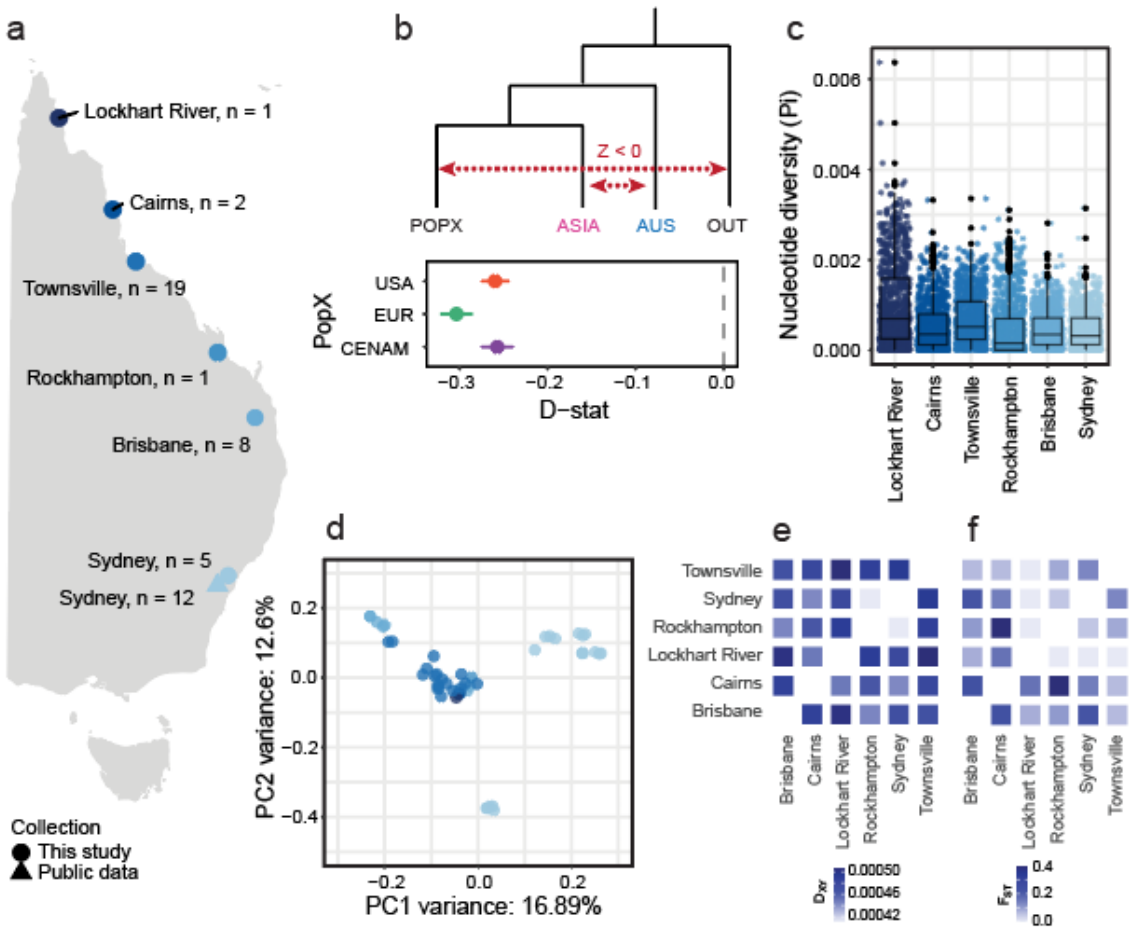

Fig. 5: Gene flow and population structure of Australian heartworms. a, Distribution of adult heartworm samples (*n* = 48) collected along the east coast of Australia. **b,** *D*-statistics showing excessive allele sharing between Australia (AUS) and ASIA relative to that between AUS and other regions (PopX). Admixtools qpDstat was used to analyse 21,088 single nucleotide polymorphisms (SNPs), with *Dirofilaria ursi* as the outgroup (OUT). *D*-statistics test for admixture between four populations (W, X, Y, Z). A Z-score (*D*-statistic / standard error) is calculated, which provides information about the direction of gene flow (red dotted lines) (Z-score > 0 = gene flow between [W and Y], or [X and Z]; Z-score < 0 = gene flow between [W and Z] or [X and Y]). For all data presented, the Z score was significant (|Z| > 3). Error bars show the standard error. **c,** Box plots showing the nucleotide diversity (Pi)

855 distribution from dog hosts per city. Each data point represents a 100 kb sliding window. **d,**

856 Principal component analysis (PCA) of 116,492 nuclear SNPs in the Australian cohort. **e**,

857 Absolute nucleotide divergence (D_{XY}) and **f,** genetic differentiation (F_{ST}) between Australian

858 cities using a median of 100 kb sliding windows. Only heartworms from dog hosts were

859 included in the analysis.

860

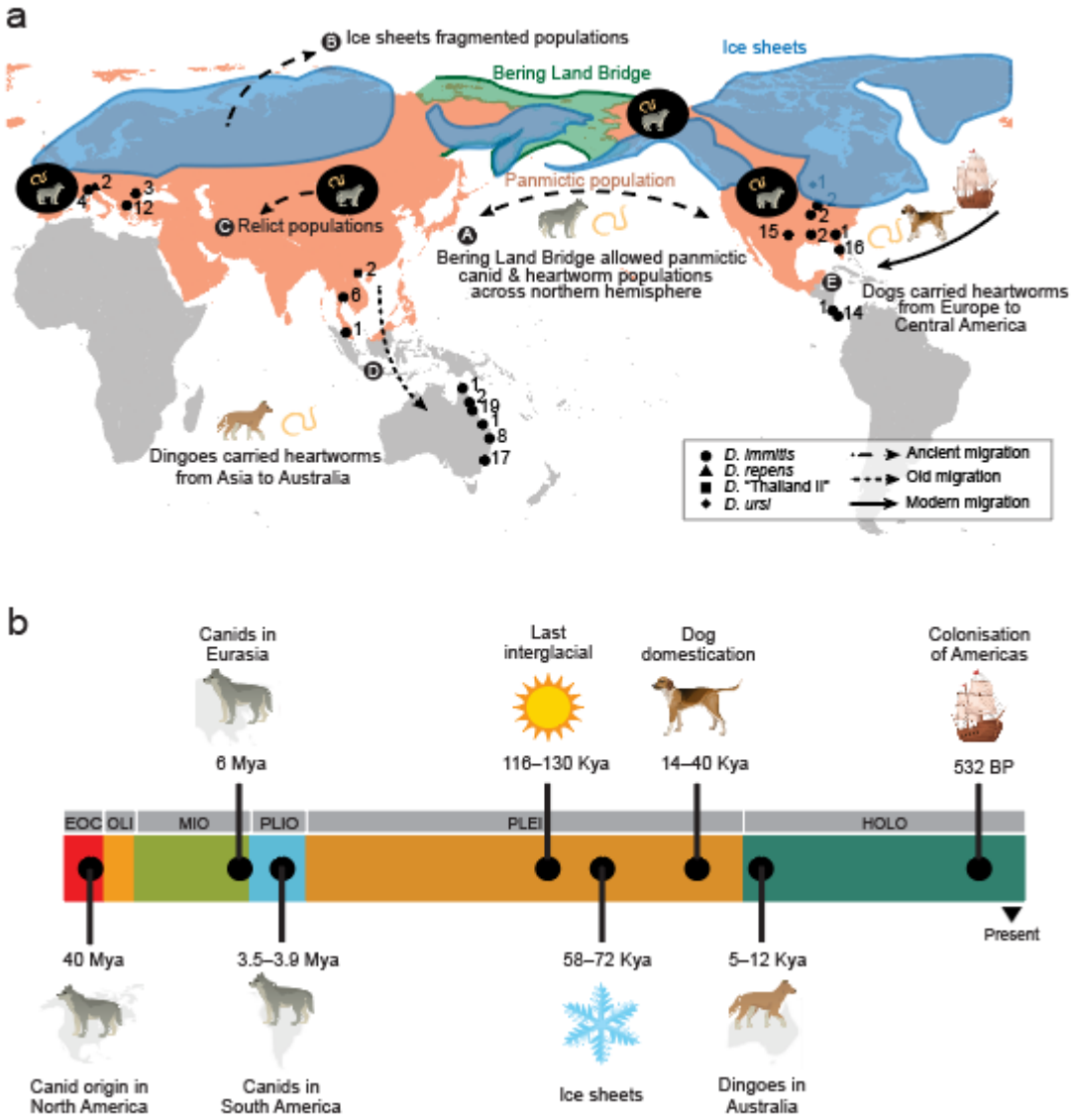

Fig. 6: A new evolutionary paradigm of heartworms throughout history. a, Hypothetical heartworm dispersal scenarios supported in the current study. Pink regions represent a panmictic population of ancient canids harbouring heartworms across North America and Eurasia. The Bering Land Bridge is shaded in green, and continental ice sheets are shown in blue. Events are in chronological order (A–E), with arrows illustrating ancient (dashed), old (dotted), and modern (solid) migration events. Small black shapes with adjacent numbers indicate the geographic origin of samples collected in this study and their sample size. The

legend specifies the parasite species, including the heartworm *Dirofilaria immitis* (*n* = 127) and outgroups *D. repens* (*n* = 2), *D*. sp. 'Thailand II' (*n* = 2), and *D. ursi* (*n* = 1). **b,** Timeline of key canid evolution and climatic events. Horizontal bars represent Epochs: HOLO = Holocene; PLEI = Pleistocene; PLIO = Pliocene; MIO = Miocene; OLI = Oligocene; EOC = Eocene. The time scale was log-transformed to enhance the visualisation of events.